Article

Not peer-reviewed version

Small Intestine Neuromuscular Dysfunctions and Neurogliopathy in a Mouse Model of High-Fat Diet-Induced Obesity: Involvement of Toll-Like Receptor 4

Sofia Faggin , Silvia Cerantola , Annalisa Bosi , Cristina Giaroni , Eleonora Napoli , Edoardo Vincenzo Savarino , Carolina Pellegrini , Luca Antonioli , Valentina Caputi * , Maria Cecilia Giron *

Posted Date: 26 June 2025

doi: 10.20944/preprints202506.2222.v1

Keywords: obesity; Toll-like receptor 4; high-fat diet; enteric nervous system; serotonin; inflammation; neurodegeneration

 doi:10.20944/preprints202506.2222.v1

Article

Small Intestine Neuromuscular Dysfunctions and Neurogliopathy in a Mouse Model of High-Fat Diet-Induced Obesity: Involvement of Toll-like Receptor 4

Sofia Faggin [1,†], Silvia Cerantola [1,†], Annalisa Bosi [2], Cristina Giaroni [2], Eleonora Napoli [3], Edoardo V. Savarino [4], Carolina Pellegrini [5], Luca Antonioli [5], Valentina Caputi [6,*] and Maria Cecilia Giron [1,*]

[1] Department of Pharmaceutical and Pharmacological Sciences, University of Padova, 35131 Padova, Italy
[2] Department of Medicine and Surgery, University of Insubria, Varese, Italy
[3] Department of Neurology, School of Medicine, University of California Davis, Sacramento, CA, USA
[4] Department of Surgery, Oncology and Gastroenterology, University of Padova, Padova, Italy
[5] Department of Clinical and Experimental Medicine, University of Pisa, Pisa, Italy
[6] Department of Poultry Science, University of Arkansas, Fayetteville, AR, USA
* Correspondence: cecilia.giron@unipd.it (M.C.G.); vcaputi@uark.edu (V.C.)
† Authors contributed equally to this study.

Abstract

Obesity is associated to enteric dysfunctions, such as gut dysmotility and neurodegeneration, potentially involving Toll-like receptor 4 (TLR4) signaling. Therefore, we assessed the impact of TLR4 deficiency on small intestine enteric nervous system (ENS) in a mouse model of high-fat diet (HFD)-induced obesity.TLR4$^{-/-}$ and wild-type (WT) C57BL/6J male mice (aged 9±1 weeks) were fed with standard-diet (SD; 18% kcal fat) or HFD (60% kcal fat) for 8 weeks. ENS sufferance was studied by real-time qPCR and confocal immunofluorescence microscopy in longitudinal muscle-myenteric plexus whole-mount preparations. Alterations in gut motility were evaluated by stool frequency, transit of a fluorescent-labelled marker and isometric motor responses of ileal preparations to receptor and non-receptor-mediated stimuli. In WT mice, HFD caused delayed gastrointestinal transit, impairment of both cholinergic- and nitrergic-mediated responses and changes in concentration-effect curve to exogenous 5-HT. These functional alterations were associated with disrupted neuroglial network, myenteric neurodegeneration, loss of ChAT^{+} and nNOS^{+} neurons and increased 5-HT ileal tissue levels. TLR4 deficiency protected against body weight gain and prevented mostly ENS morpho-functional anomalies following HFD. Our study further supports the involvement of TLR4 in the modulation of small intestine inflammation and ENS morpho-functional changes associated with obesity.

Keywords: obesity; toll-like receptor 4; high-fat diet; enteric nervous system; serotonin; inflammation; neurodegeneration

1. Introduction

High-fat diet (HFD) is a well-established contributor to the development of overweight or obesity, conditions that currently affect over one-third of the global population and are projected to exceed 50% by 2030 [1]. Obesity, characterized by an imbalance between energy intake and expenditure, is a multifactorial and complex disease, associated with chronic, low-grade inflammation involving multiple tissues, including the gastrointestinal (GI) tract [2,3]. Adipocytes and adipose tissue-associated macrophages have long been recognized as major sources of pro-inflammatory mediators, including several interleukins, tumor necrosis factor (TNF), and monocyte chemoattractant protein 1 (MCP-1) [4]. This pro-inflammatory state is a key driver in the

 doi:10.20944/preprints202506.2222.v1

development of various comorbidities, such as type 2 diabetes mellitus, cardiovascular diseases, cognitive decline, dementia and certain cancers [5,6].

Emerging clinical evidence has highlighted a strong association between obesity and chronic GI disturbances, including gastroesophageal reflux, diarrhea and constipation, which further impair patients' quality of life [7,8]. Preclinical studies have shown that chronic exposure to HFD leads to increased intestinal permeability and gut inflammation, impairing the ENS with consequent disruption of gut motor function [2,7,9,10]. The increased permeability favors the translocation of bacterial endotoxins, promoting low-grade inflammation and metabolic disorders [11]. HFD alters the gut microbiota composition, typically marked by an increased Firmicutes-to-Bacteroidetes ratio. This dysbiotic state has been linked to higher energy harvest from the diet and contributes to obesity development [12,13]. Conversely, HFD consumption has been shown to affect intestinal transit time, with some studies reporting accelerated colon transit [14] and others showing delayed transit [13]. These conflicting results suggest that the effects may depend on the duration and composition of the HFD [14].

Toll-like receptors (TLRs) represent a class of pattern-recognition receptor family that recognize pathogen- and damage-associated molecular patterns and activate innate immune responses. Among TLRs, TLR4 induce innate immune responses when stimulated by lipopolysaccharides (LPS), main component of the outer membrane of Gram-negative bacteria [15,16]. Beyond immunity, TLR4 signaling influences ENS homeostasis and GI function [16,17]. In normal conditions, TLR4$^{-/-}$ mice have shown altered gut motility and changes in small intestinal and colonic ENS neuronal populations [16–20] and to be protected from obesity-induced inflammation and insulin resistance [21–23]. HFD appears to not affect GI transit and colonic myenteric cell number in TLR4$^{-/-}$ mice, highlighting the importance of TLR4 signaling in enteric neuroinflammation and motility disturbances in diet-induced obesity models [13,21,22,24]. Despite these advances, the impact of HFD on small intestinal contractility, neurotransmission pathways and integrity of myenteric nervous system in absence of TLR4 signaling remains still unclear. Elucidating the role of TLR4 in modulating ENS circuitries in response to dietary fat could enhance our understanding of the mechanisms linking diet, immune signaling, and GI motility. Such a possibility was addressed in the present study by short-term 8-week high fat diet-feeding of WT and TLR4$^{-/-}$ mice. We found that HFD delayed GI transit, impaired excitatory cholinergic and inhibitory nitrergic neurotransmission and serotonergic response and metabolism, which were mostly prevented by TLR4 deficiency.

2. Results

2.1. Influence of TLR4 Signaling on HFD-Induced Obese Phenotype

To confirm that HFD consumption recapitulates the classic signs of obesity, we monitored the body weight gain, blood metabolic parameters and ileal levels of inflammatory mediators in both genotypes during HFD or SD administration. After 8 weeks, HFD determined a significant body weight gain in both WT and TLR4$^{-/-}$ mice (+28% and +10%, respectively; **Figure 1A,B**) compared to that of SD-fed mice. Interestingly, in TLR4$^{-/-}$ mice the increase in body weight occurred at the week 5 of HFD treatment, whereas in WT mice this increase was observed from the beginning of HFD exposure. Higher plasma levels of glucose, triglycerides, and cholesterol (+20%, +48% and +40%; respectively; **Figure 1C–E**) were found in WT HFD mice compared to the SD group, as previously reported [25]. In TLR4$^{-/-}$ mice, HFD induced a marked increase in triglycerides and cholesterol (+58% and +25%, respectively; **Figure 1C,D**) without altering glucose levels (**Figure 1E**). To investigate whether HFD consumption might determine gut inflammation, we measured proinflammatory gene expression in small intestinal mucosa-deprived tissue from 8-week fed SD and HFD mice of both the genotypes. We found a 1.8-fold, 5.1-fold and 1.1-fold increase in TNFα, IL-1β and IL-6 mRNA levels, respectively, (**Figure 1F–H**) in WT HFD mice compared to related SD animals, indicating the presence of an inflammatory state in the small intestine neuromuscular compartment, as observed previously in the colon of HFD mice [13,21]. In SD condition, TLR4$^{-/-}$ mice exhibited high proinflammatory

 doi:10.20944/preprints202506.2222.v1

cytokines gene expression compared to WT SD mice, which, surprisingly, resulted not affected by 8-week HFD (**Figure 1F–H**).

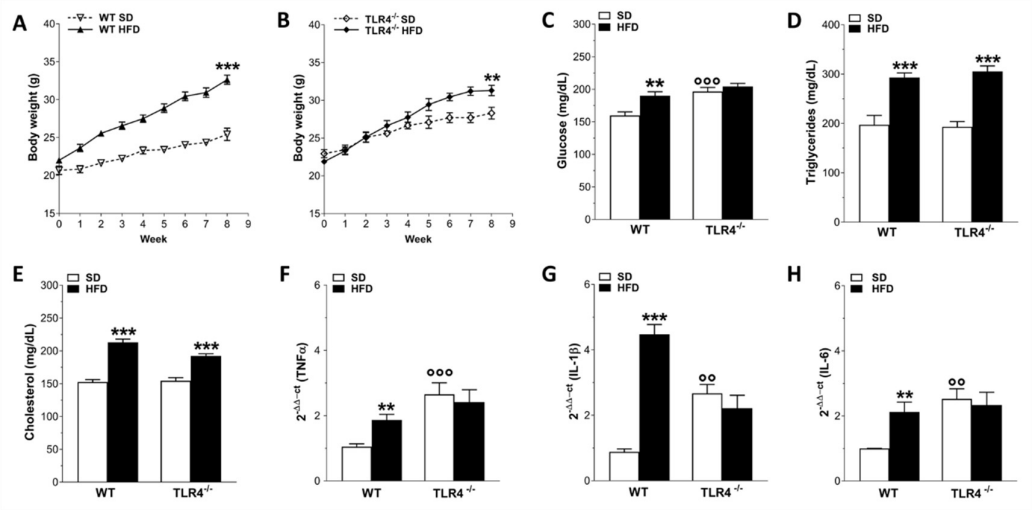

Figure 1. Phenotypic changes and inflammation marker levels after HFD-induced obesity. A,B) Body weight gain in WT **(A)** and TLR4$^{-/-}$ **(B)** mice after 8 weeks of HFD treatment; N=20 mice/group. **C-E)** Glucose **(C)**, cholesterol **(D)**, triglycerides **(E)** plasma levels in WT and TLR4$^{-/-}$ mice fed with SD or HFD; N=20 mice/group. **F-H)** Real-time PCR analysis of TNFα **(F)**, IL-1β **(G)** and IL-6 **(I)** mRNA levels in ileal tissues from WT and TLR4$^{-/-}$ mice fed with SD or HFD; N=5 mice/group. **P<0.01, ***P<0.001 vs related SD genotype; °°P<0.01, °°°P<0.001 vs WT SD mice.

2.2. TLR4 Signaling Is Involved in HFD-Induced Gastrointestinal Dysmotility

Several studies on HFD animal models have reported that obesity contributes to the development of constipation, generally observed in obese patients [7]. Therefore, we evaluated the GI transit as well as the fecal pellet output and related water content to uncover any changes in entire enteric motor propulsive activity and barrier function. As we previously revealed [16], TLR4$^{-/-}$ SD mice displayed a significant reduction of the geometric center (GC) compared to WT mice ($GC_{WT\ SD}$=6.9 vs $GC_{TLR4\text{-}/\text{-}\ SD}$=6.2; **Figure 2A–C**) associated to a delayed gastric emptying, decreased fecal pellets/hour and stool water content (**Figure 2D–F**). However, only in WT mice HFD prolonged the GI transit time, as showed by the marked reduction of the GC compared to SD-fed mice ($GC_{WT\ SD}$=6.9 vs $GC_{WT\ HFD}$=5.5; **Figure 2A,C**). Furthermore, reduced gastric emptying, stool expulsion frequency and fecal water content were also observed in WT HFD mice (**Figure 2D–F**). In both genotypes, HFD significantly impaired stomach and caecum weight (**Figure 3A,B**), as well as small intestine and colon length (**Figure 3C,D**).

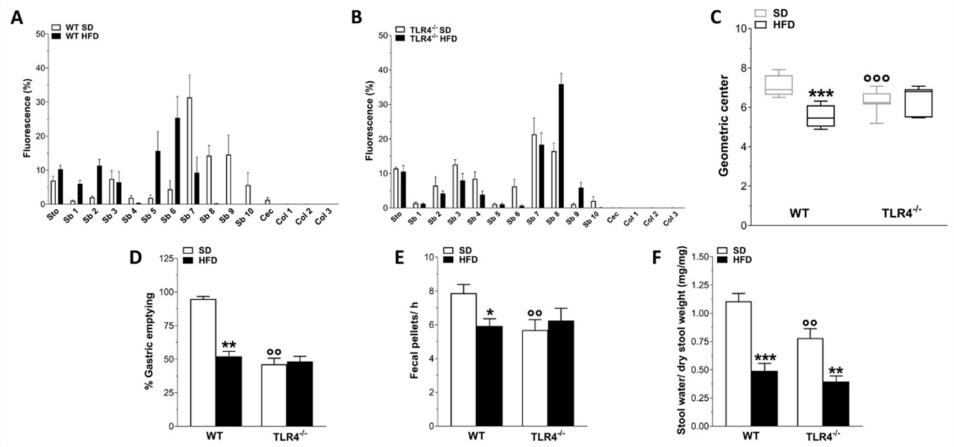

 doi:10.20944/preprints202506.2222.v1

Figure 2. TLR4 signaling influenced HFD-effects on gastrointestinal motility. A,B) Distribution of the non-absorbable FITC dextran 70 kDa, reported as % fluorescence ± SEM in the individual segments of the digestive tract (Cec, caecum; Col1–Col3, colon segments; Sb1–Sb10, small bowel segments; Sto, stomach) in WT **(A)** and TLR4$^{-/-}$ **(B)** mice fed with SD or HFD; N = 10 mice/group. **C)** Geometric center calculated following the analysis of the GI transit, reported as median with its percentile; N = 10 mice/group. **D-F)** Percentage of gastric emptying **(D)**, total number of fecal pellets expelled in 1-hour collection period **(E)** and stool water content **(F)** from WT and TLR4$^{-/-}$ mice fed with SD or HFD; N=10 mice/group. Data are reported as mean ± SEM. *P<0.05, **P<0.01 , ***P<0.001 vs related SD genotype; °°P<0.01, °°°P<0.001 vs WT SD mice.

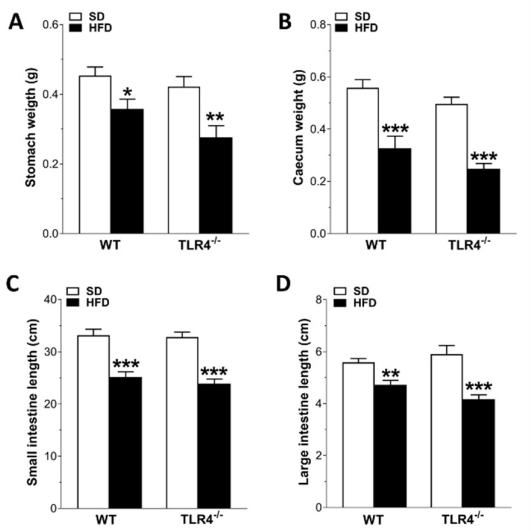

Figure 3. HFD affected gastrointestinal tract morphology. Changes in stomach **(A)** and caecum **(B)** weights, as well as in small **(C)** and large intestine **(D)** lengths in WT and TLR4$^{-/-}$ mice fed with SD or HFD. Data are reported as mean ± SEM. *P<0.05, **P<0.01, ***P<0.001 vs related SD genotype; N=20 mice/group.

2.3. TLR4 Signaling Influences Small Intestine Excitatory Cholinergic Neurotransmission Following 8-Week HFD

Since HFD exposure delayed the GI transit, we evaluated the excitatory neuromuscular function of isolated ileal preparations from WT and TLR4$^{-/-}$ mice, by analyzing the cumulative concentration-response curves to the non-selective cholinergic receptor agonist CCh. After 8 weeks of HFD, WT mice showed a significant downward shift of the concentration-response curve to CCh and a related significant decrease of the maximum contraction compared to controls mice (Emax=-32%; **Figure 4A**). As previously reported by our group [16], TLR4$^{-/-}$ SD mice exhibited a lower CCh-mediated contraction compared to WT animals (**Figure 4A**), which was not altered following HFD treatment. In both genotypes, HFD-induced obesity caused a significant decrease of EFS-elicited contractions, as shown by the reduced maximum response at 40 Hz (-42% in WT and +34% in TLR4$^{-/-}$; **Figure 4B**).

In the mouse ileum, EFS-mediated responses to frequencies up to 10 Hz are of neuronal cholinergic origin, being sensitive to both TTX and atropine[26]. Intriguingly, 10 Hz-EFS-mediated responses determined a significant reduction of cholinergic contraction only in ileal segments of WT HFD mice compared to WT SD mice (-33%; **Figure 4B**), indicative of alterations in enteric cholinergic neurotransmission. Therefore, we evaluated the immunoreactivity of the enzyme ChAT in the myenteric plexus of WT and TLR4$^{-/-}$ mice (**Figure 5**), to assess the status of ileal cholinergic network. HFD administration caused a significant reduction of ChAT immunofluorescence (-14%) and disrupted architecture of myenteric cholinergic network (**Figure 5**) only in WT mice compared to WT SD mice, without any alterations in the TLR4$^{-/-}$ group, confirming the involvement of TLR4 signaling in the impairment of cholinergic neuromuscular response.

 doi:10.20944/preprints202506.2222.v1

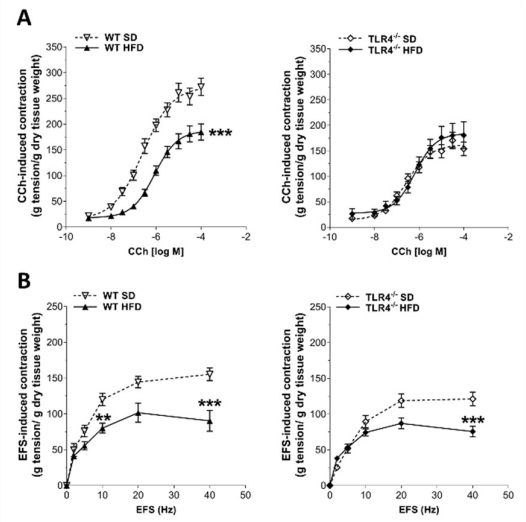

Figure 4. HFD impaired the enteric cholinergic excitatory response in WT mice. A) Concentration–response curves to carbachol (CCh; 0.001 – 100 μM) and **(B)** neuronal excitatory response induced by EFS (0–40 Hz) in isolated ileal preparations from WT and in TLR4$^{-/-}$ mice fed with SD or HFD. Data are reported as mean ± SEM. **P<0.01, ***P<0.001 vs related SD genotype. N=10 mice/group.

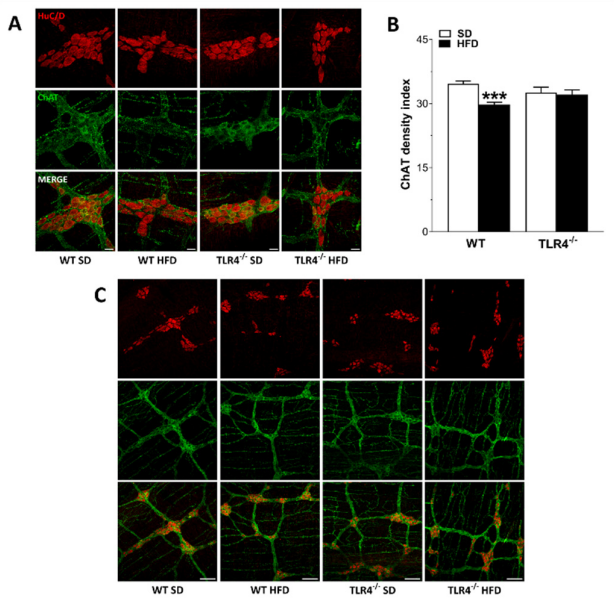

Figure 5. HFD affected the myenteric cholinergic network in WT mice. A,C) Representative confocal microphotographs [magnification 63x **(A)** or 20x **(C)**] showing the distribution of ChAT (green, marker for cholinergic neurons) and HuC/D (red, pan-neuronal marker) in LMMP preparations from of WT and TLR4$^{-/-}$ mice fed with SD or HFD; scale bars = 20 μm **(A)** or 100 μm **(C)**. **B**) ChAT density index in LMMP preparations of WT and TLR4$^{-/-}$ mice fed with SD or HFD. Data are reported as mean ± SEM. ***P<0.001 vs related SD genotype. N=5 mice/group.

2.4. TLR4 Signaling Affects Ileal Inhibitory Nitrergic Neurotransmission During HFD

Considering that the reduced excitatory contraction could be the result of an increased inhibitory tone, we assessed ileal nitrergic neurotransmission. As previously shown [16], in NANC conditions EFS at 10 Hz caused a 1.3-fold increase in relaxation sensitive to the iNOS inhibitor 1400W and to the pan-NOS inhibitor L-NAME in TLR4$^{-/-}$ mice preparations whereas in WT segments EFS-evoked NANC relaxation was almost completely blocked by L-NAME (**Figure 6A,B**). Upon HFD, WT mice

 doi:10.20944/preprints202506.2222.v1

displayed a significant reduction in the inhibitory response compared to WT SD mice (by 26±1%; **Figure 6A**). The pre-treatment with 1400W determined a slight but not significant reduction of the NANC-mediated relaxation (**Figure 6A**). Pre-treatment with L-NAME almost completely blocked EFS-evoked NANC relaxation in WT mice fed with SD or HFD (**Figure 6A**). On the other hand, 8 weeks-treatment with HFD determined a significantly reduction of the inhibitory response of TLR4$^{-/-}$ ileal preparations compared to those from TLR4$^{-/-}$ SD animals (by 24±2%; **Figure 6B**). The addition of 1400W did not change the NANC-mediated relaxation obtained in TLR4$^{-/-}$ HFD mice (**Figure 6B**), suggesting that TLR4 deficiency protects against the development of a low-grade inflammatory state caused by HFD, as previously shown in TLR4$^{-/-}$ mice [21]. Pre-treatment with L-NAME almost completely blocked EFS-evoked NANC relaxation of ileal samples from TLR4$^{-/-}$ HFD mice (**Figure 6B**), reaching an inhibitory response comparable to that found in WT SD mice. TLR4$^{-/-}$ SD myenteric ganglia showed a significant reduction of nNOS^{+} neurons (by -26±1%; **Figure 6C,E**) compared to WT SD mice. After HFD, the number of nNOS^{+} neurons decreased by 23% in myenteric ganglia of WT mice (**Figure 6C,E**), with slight but not significant changes in LMMPs of TLR4$^{-/-}$ mice. Moreover, HFD caused neuronal loss only in WT mice (**Figure 6C,D**), confirming the results obtained by others in the large [13,27] and small intestine [28,29].

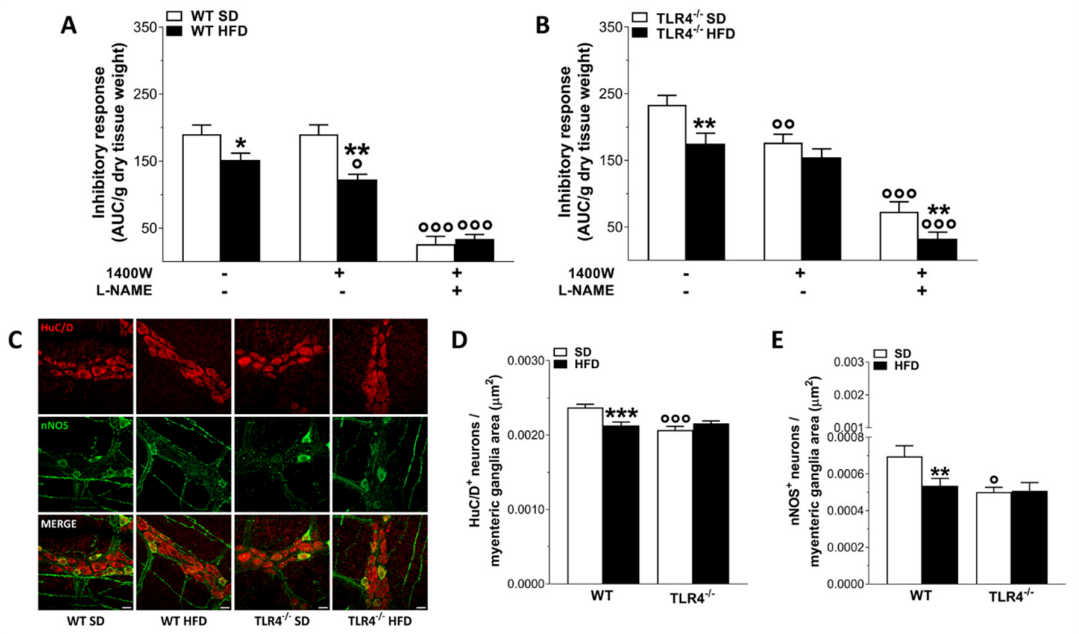

Figure 6. TLR4 signaling influenced HFD-induced enteric neurodegeneration, modulating also NO-mediated relaxation. (A-B) 10 Hz EFS-evoked relaxation in NANC conditions with or without 10 μM 1400 W (iNOS inhibitor) or 100 μM L-NAME (pan-NOS inhibitor) in ileal segments of WT **(A)** and TLR4$^{-/-}$ **(B)** mice fed with SD or HFD; N=10 mice/group. *P<0.05, **P<0.01 vs related SD genotype; °P<0.05, °°P<0.01, °°°P<0.001 vs respective control in NANC conditions. **C)** Representative confocal microphotographs showing the distribution of HuC/D (red) and nNOS (green) and **(D,E)** analysis of HuC/D^{+} and nNOS^{+} neurons in ileal LMMPs of WT and TLR4$^{-/-}$ mice fed with SD or HFD (scale bars = 20 μm). Data are reported as mean ± SEM. *P<0.05, **P<0.01 , ***P<0.001 vs related SD genotype; °P<0.05, °°°P<0.001 vs WT SD mice.

3.5. HFD Affects Enteric Neuroplasticity in a TLR4-Dependent Manner

For assessing the effect of diet on ENS structure we evaluated the number of HuC/D^{+} neurons and the distribution of the glial markers S100β and GFAP. Higher immunoreactivity and expression of the glial markers GFAP and S100β are indicative of ENS neuroplasticity and reactive gliosis [19,20,30]. We have previously shown that, the absence of TLR4 signaling caused a significant increase of S100β and GFAP density index, indicative of inflammation in EGCs compared to that found in WT SD mice (+79±2% and +15±1%, respectively; **Figure 7**) [20]. Furthermore, TLR4$^{-/-}$

 doi:10.20944/preprints202506.2222.v1

myenteric ganglia showed a significant reduction of the total number of HuC/D$^+$ neurons (-12±1%) compared to WT mice in SD (-9±2%).

HFD administration determined reactive gliosis in WT mice, causing 2.4-fold increase of S100β immunoreactivity together with 1.2-fold increase of GFAP immunoreactivity, respectively (**Figure 5**). In TLR4$^{-/-}$ mice, HFD appears to normalize enteric gliosis reducing S100β and GFAP immunoreactivity (-25±2%, -33±2%, respectively; **Figure 7**). All together these data suggest an involvement of TLR4 signaling in the development of small intestine neuro-gliopathy induced by HFD.

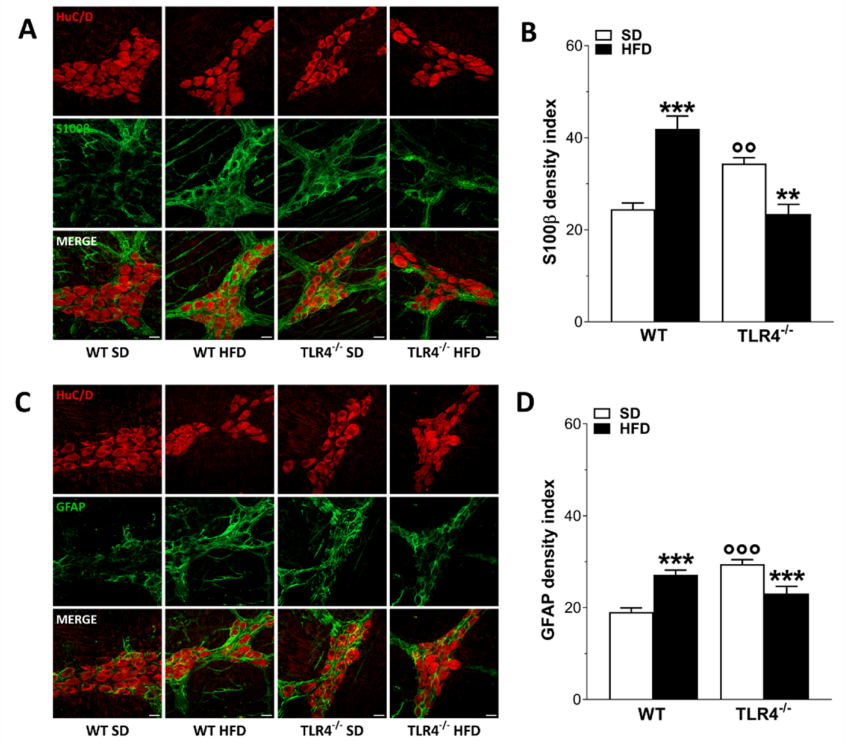

Figure 7. HFD-induced obesity determined neuroplastic changes in myenteric plexus architecture of WT mice. (A,C) Representative confocal microphotographs showing the distribution of HuC/D$^+$ (red) neurons and S100β$^+$ (green, **A**), and glial fibrillary acidic protein (GFAP)$^+$ (green, **C**) glial cells in longitudinal muscle–myenteric plexus (LMMP) preparations of WT and TLR4$^{-/-}$ mice fed with SD or HFD (scale bars = 20 μm). **(B,D)** Analysis of S100β **(B)** and GFAP **(D)** fluorescence intensity index in LMMP preparations of WT and TLR4$^{-/-}$ mice fed with SD or HFD; N=5 mice/group. Data are reported as mean ± SEM. **P<0.01 , ***P<0.001 vs related SD genotype; °°P<0.01, °°°P<0.001 vs WT SD mice.

3.6. TLR4 Deficiency Affects 5-HTergic Neurotransmission Following HFD-Induced Obesity

Considering the impact of 8-week HFD on cholinergic- and nitrergic-mediated neuromuscular response in WT HFD mice, we decided to evaluate the role of 5-HT in ileal contractility of mice fed with SD or HFD. Studies in mice and rats have shown that after HFD the level of 5-HT is increased probably due to an inhibitory effect on food intake and body weight gain [31,32]. In ileal tissues from TLR4$^{-/-}$ mice, 5-HT levels were significantly higher than in WT mice (**Figure 8A**). Upon HFD treatment, 5-HT levels were significantly increased in WT mice but not in TLR4$^{-/-}$ animals (**Figure 8A**).It is known that 5-HT activates both intrinsic excitatory and inhibitory enteric motor neurons [33]. Isolated ileal preparations from WT and TLR4$^{-/-}$ mice fed with SD were incubated with increasing concentrations of 5-HT to obtain a non-cumulative concentration-response curve. As shown in **Figure 8B**, in WT HFD mice ileal contraction resulted significantly increased following the addition of exogenous 0.3 μM 5-HT whereas resulted comparable to the response obtained from SD ileal

 doi:10.20944/preprints202506.2222.v1

segments incubated to higher 5-HT concentrations. In TLR4$^{-/-}$ mice fed with SD a higher 5-HT-induced contraction was observed, as shown by the significant upward shift of the concentration–response curve to 5-HT (**Figure 8C**). HFD administration determined a significantly reduction of the 5-HT-mediated response compared to TLR4$^{-/-}$ SD mice (**Figure 8C**).

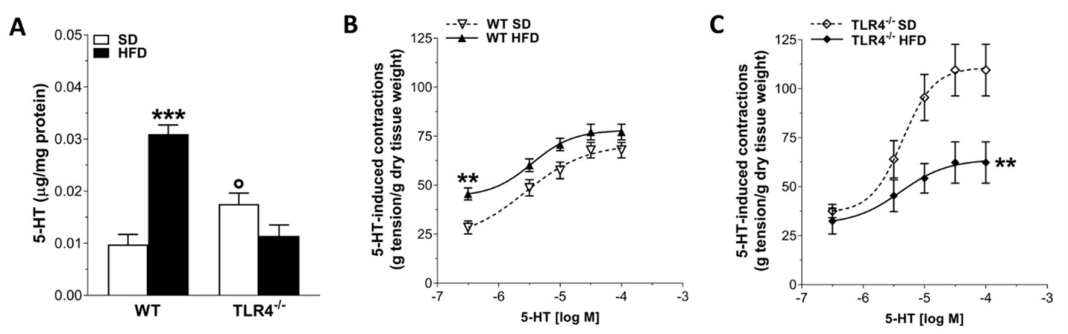

Figure 8. HFD-induced obesity altered 5-HT-mediated ileal contraction in TLR4$^{-/-}$ mice. (A) 5-HT levels measured by HPLC analysis in ileal tissues of WT and TLR4$^{-/-}$ mice fed with SD or HFD; N=5 mice/group. **(B,C)** Non-cumulative concentration response curves to 5-HT (0.3–100 µM) of isolated ileal preparations from WT and TLR4$^{-/-}$ mice fed with SD or HFD; N=10 mice/group. Data are reported as mean ± SEM. **P<0.01, ***P<0.001 vs related SD genotype; °P<0.05 vs WT SD mice.

3. Discussion

A diet rich in fatty food is known to determine a chronic systemic mild inflammation causing changes in gut motility, mainly constipation in humans and animal models, evidenced by slow intestinal propulsive activity [7,34]. Indeed, the presence of low-grade systemic inflammation associated with obesity usually involves a complex network of signals, including gut-microbiota-dependent pathways, which may influence several organs (e.g., brain function, behavior). However, the causal pathways between obesity, inflammation, neurodegeneration and metabolic disease remain not completely understood [35]. The 60% lipid content in HFD mimics a contemporary diet based in a high-fat, low-carbohydrate diet in humans, which determines body weight gain and dysmetabolic features, characteristic of moderate obesity [13]. Its consumption for more than 4 weeks showed delayed gastrointestinal transit associated with ganglionic shrinkage, reduced nerve cell soma, lower number of nitrergic neurons always in the colon, to highlight an association between gut dysmotility and enteric neuropathy [13,22,25,28,36]. However, the molecular mechanisms underlying obesity-induced colonic dysmotility and enteric neuropathy are still not fully clarified.

Although the effects of obesity on the central and hormonal control of GI motility have been well documented in colonic tissues only few studies have explored the effects of HFD and TLR4 deficiency on ENS activity of the small intestine [7,21,22,25,29]. The small intestine is recognized to own the largest population of enteric neurons and to be essential for nutrient absorption and immune, neural and endocrine responses[37]. TLR4 activity is influenced by dietary components: saturated fatty acids can activate its signaling to mediate inflammatory processes, whereas unsaturated fats may exert an opposing, anti-inflammatory effect [38]. Several studies on HFD-induced obesity showed that HFD determines impaired GI transit, increased plasma LPS concentrations and TLR4-mediated release of proinflammatory cytokines and myenteric neurons apoptosis primarily in the colon [13,22].

In this study, we have characterized, for the first time, the impact of TLR4 signaling in small intestine ENS morpho-functional integrity in a murine model of 8-week HFD-induced obesity. Specifically, the novel findings of this study demonstrate that HFD-induced obesity determines in the small intestine the following effects dependent on TLR4 signaling: (i) delayed GI transit; (ii) complex abnormalities in enteric neuroglioplasticity; (iii) impaired excitatory cholinergic neuromuscular responses; (iv) reduced intestinal inhibitory motor tone, partially sustained by

 doi:10.20944/preprints202506.2222.v1

enhanced iNOS- and nNOS-derived NO; (v) myenteric neurodegeneration and loss of nNOS$^+$ neurons and (vi) altered 5-HT-mediated neuromuscular response and 5-HT ileal content.

After 8 weeks of HFD WT mice developed obesity together with significant changes in metabolic indexes (i.e., increase in blood glucose, triglycerides and cholesterol), thus substantiating the appropriateness of this model as previously shown [6,39]. Although the macroscopic assessment score did not evidence any substantial difference between the experimental groups, HFD caused intestinal a low-grade inflammation, manifested by shortening of the GI tract, and increased expression of TNFα, IL-1β, and IL-6. Several studies have shown that HFD animals exhibited a higher expression of pro-inflammatory cytokines (TNF, IL-1β, IL-6) in intestinal tissues, together with modified organ morphology, altered mucin biosynthesis and impaired mucosal barrier, suggesting a key role of obesity in the onset of gut inflammation and altered permeability [21,22,40].

Conversely, only after 5 weeks of HFD TLR4$^{-/-}$ mice reached a body weight significantly different from that one of mice fed with SD, associated to changes in lipid profile and gut morphology parameters. However, HFD had no effect on glycemia and mRNA levels of mucosa-deprived proinflammatory cytokines, as previously shown in the colon [21]. HFD caused a marked decrease in transit time and stool water content in WT mice, with no changes in TLR4$^{-/-}$ mice suggesting that the absence of TLR4 signaling partially protects against the HFD-induced constipation, possibly due to changes in gut microbiota and ENS activity. TLR4 has, indeed, emerged as an interesting link between inflammation and insulin resistance. Beside LPS, TLR4 can be activated by saturated free fatty acids during hyperlipidemic state associated with obesity and secondary to long-term ingestion of a HFD [23,41]. TLR4 mutations or deficiency have been shown to partially protect against the detrimental metabolic effect of obesity [23,38,42]. Gut inflammation begins when TLR4 stimulation, following the binding of its own ligands such as LPS or other PAMPs, determines the activation of NF-κB causing the production of different cytokines including TNFα and IL-1β [4]. Recent studies have demonstrated that inflammation leads to several changes in the neuron's circuitry, causing alterations in the hyperexcitability of neurons, peristaltic reflex, synaptic facilitation, and attenuated inhibitory neuromuscular transmission, leading to constipation that is one of the main features of obesity [7,24].

Indeed, we found a marked reduction in the neuromuscular excitatory cholinergic response following 8-week HFD in WT with no difference in TLR4$^{-/-}$ mice. These impairment in cholinergic neurotransmission could be ascribed to the presence of cholinergic neural sufferance, as shown by the reduction in ChAT$^+$ neurons. Since the loss of ChAT$^+$ neurons in proximal colon of mice fed with HFD have been observed previously [14,25,43], our findings further highlight a critical role of TLR4 signaling in neuronal plasticity as confirmed by the immunofluorescence results.

To characterize the effects of these cholinergic anomalies on neuromuscular contractility, we evaluated the NANC-mediated relaxation in isolated ileal segments from both genotypes after HFD. In absence of inflammation WT mice showed an inhibitory response mediated by only nNOS activity, whereas TLR4$^{-/-}$ mice had an inhibitory response mediated by both iNOS and nNOS [16]. After development of obesity, we found in WT mice a reduced inhibitory tone affected by nNOS and iNOS-produced NO, being significantly different compared to the response in SD condition, suggesting the presence of a low-grade inflammation and loss of nNOS neurons as previously shown in the gastrointestinal tract [2,21,28,44]. TLR4$^{-/-}$ mice fed with HFD showed no changes in the nitrergic pathways but a reduction of inhibitory response possibly due to other inhibitory pathways [16]. No change in iNOS expression, even if not significative, has been previously shown in the colon of TLR4$^{-/-}$ mice fed with HFD [21], to further suggest that changes in the gut microbiota determined by HFD may play a pivotal role in the induction of LPS-induced inflammatory status in the intestine and may contribute to the phenotype observed in HFD mice.

In response to injury, stress, or inflammation, EGCs, located in the myenteric ganglia, become reactive as shown by the upregulation of their markers S100β and GFAP [19,20].

In agreement with previous findings [6,10,39], we revealed an increase of S100β and GFAP immunofluorescence in WT mice after HFD. Conversely, in TLR4$^{-/-}$ myenteric ganglia HFD

 doi:10.20944/preprints202506.2222.v1

determined a marked reduction in GFAP and S100β. These data further support the involvement of TLR4 pathway not only in the control glial commitment but also in neurodegeneration, both in colon and small intestine [13,16,20,22].

The role of 5-HT in GI disorders is still controversial and several studies have suggested a relationship between the serotonergic system, obesity and IBD (Bertrand et al., 2012; Mawe & Hoffman, 2013). In the ileum of TLR4$^{-/-}$ mice, 5-HT-evoked contractile response resulted significantly increase compared to WT mice, associated to higher content in 5-HT in ileal mucosa-deprived specimens, advocating the presence of an interactive dialogue between the intestinal serotonergic neurotransmission and TLR4 [19,45,46]. HFD did change only 5-HT ileal tissue only in WT mice, suggesting the presence of a low-grade gut inflammation as well as affected ileal neuromuscolar response, to further suggest an involvement of TLR4 signaling in small intestine dismotility in presence of obesity, as previously shown [31,32].

4. Materials and Methods

4.1. Mice

Experiments were achieved using male TLR4$^{-/-}$ (B6.B10ScN-Tlr4$^{lps\text{-}del}$/JthJ) mice aged 9 ± 1 week old and sex- and age-matched wild-type (WT) C57BL/6J mice (Jackson Laboratories, Bar Harbor, ME, United States). All animals were housed in individually ventilated cages at the Animal Facility of the Department of Pharmaceutical and Pharmacological Sciences, University of Padova under controlled environmental conditions (temperature 22°±2°C; relative humidity 60–70%). All animals were specific pathogen-free and given standard chow diet and tap water *ad libitum* and maintained at a regular 12/12-h light/dark cycle. All experimental protocols were approved by the Italian Ministry of Health (authorization n° 1142/2015-PR and 624/2021-PR), the Animal Care and Use Ethics Committee of the University of Padova and were in compliance with ARRIVE guidelines [47–49] and with national and European guidelines for the handling and use of experimental animals.

4.2. In Vivo Treatments

To reproduce an obese status, mice TLR4$^{-/-}$ and WT were randomly divided in two groups and fed with a commercial standard diet (SD goup; provided 3.1 kcal/g, with 11% kcal as fats, 24% kcal as proteins, and 65% kcal as carbohydrates; Altromin International) with a fat-enriched diet (HFD group; provided 5.1 kcal/g, with 60% kcal as fats, 19% kcal as proteins, and 21% kcal as carbohydrates; Altromin International;[6,39]. After 8 weeks, animals were killed by cervical dislocation. All the subsequent experimental procedures were conducted blindly.

4.3. Measurement of Metabolic Parameters

Blood samples were taken from the tail vein of mice exposed to SD or HFD. After 1-hour starvation, triglycerides, cholesterol and glucose levels were measured using Multicare Insensor (BSI Srl, Arezzo, Italy), according to the manufacturer's instructions as described previously [39,50].

4.4. Gastrointestinal Transit Analysis

Fluorescein isothiocyanate (FITC)-labeled dextran (70 kDa; 100 µl of 25 mg/ml in 0.9% saline) was aministered by gavage to mice [16,26]. After 30 minutes, time needed to the fluorescent probe to reach the maximal concentration in the small intestine in physiologial conditions[19], mice were sacrificed, and the whole GI tract from stomach to distal colon was collected, measured and placed into Krebs solution. The stomach and caecum were weight and analyzed separately while the small intestine and the colon were divided into 10 and 3 segments of equal length, respectively. Tissue luminal and fecal contents were centrifuged at 12,000 rpm for 10 minutes at 4°C. FITC-dextran intensity of each segment was measured using a fluorimeter (Victor, PerkinElmer; Wallac Instruments, Turku, Finland) at excitation 485 nm and emission at 525 nm. Gastrointestinal transit

 doi:10.20944/preprints202506.2222.v1

was calculated as the geometric center (GC) of distribution of the fluorescent marker using the following formula: GC = Σ (% of total fluorescence signal per segment X segment number)/100 [26,51].

4.5. Stool Frequency and Colonic Emptying

Fecal pellet output and water content was assessed in SD and HFD non-fasted WT and TLR4$^{-/-}$ mice. Fecal water content provides an indication of constipation, diarrhea or malabsorption. Each animal was placed in a clear clean cage and was examined throughout a 60-minute period. The number of stool pellets extruded per hour (stool frequency) was used as an index of colonic emptying. Faecal pellets were collected and weighed (wet weight), subsequently dried at 65 °C for 24 h and re-weighed (dry weight). Water content was calculated from the difference in wet and dry weights and expressed as a percentage [26].

4.6. Ex Vivo Contractility Studies

Intestinal contractility was examined ex vivo by measuring tension changes on ileal samples with the isolated organ bath technique as previously described [19,20,26,52]. Distal ileal 1-cm segments from all experimental groups were isolated and mounted in organ bath containing 10 mL of oxygenated and heated (37°C) Krebs solution. Changes in ileal mechanical activity were recorded by isometric transducers (World Precision Instruments, Berlin, Germany) connected to a PowerLab 4/30 data acquisition system using LabChart 8 software (ADInstruments, Besozzo, VA, Italy). Ileal segments were subjected to an initial tension of 0.5 g and left to equilibrate for at least 45 min to allow the development of rhythmic spontaneous contractions. At the end of the equilibration period, preparations were challenged with 1 μM carbachol until stable responses were obtained (Caputi, Marsilio, Filpa, et al., 2017). To study cholinergic-mediated responses, the ileal segments were exposed to increasing concentrations of CCh (0.001-100 μM), added cumulatively, to obtain a concentration-effect curve. Neuronal-mediated contractions were obtained through electrical field stimulation (EFS, 0-40 Hz; 1-ms pulse duration; 10-s pulse-trains, 40 V) using platinum electrodes connected to a S88 stimulator (Grass Instrument, Quincy, MA, USA). Neuronal-mediated relaxations were analysed following EFS in non-adrenergic non-cholinergic (NANC) conditions (20-min preincubation with 1 μM atropine + 1 μM guanethidine). To evaluate nitrergic-mediated inhibitory neurotransmission, the effects of 100 μM Nω-nitro-L-arginine methyl ester hydrochloride (L-NAME, a non-selective nitric oxide [NO] synthase [NOS] inhibitor) or 10 μM 1400W (a selective inducible NOS [iNOS] inhibitor) were recorded on EFS-induced relaxations in NANC conditions. Concentration–response curves to 5-HT (0.3–100 μM) were obtained in a non-cumulative manner [45,53]. Contractile responses were expressed as gram tension/gram dry tissue weight of ileal segments. Inhibitory motor responses were calculated by measuring the relative area under the curve (AUC) of relaxations. The trapezoidal rule for planar area was used to obtain AUC values, which were further normalized to gram dry tissue weight [19].

 doi:10.20944/preprints202506.2222.v1

4.7. Immunohistochemistry

4.7.1. Ileal Whole Mount Preparations

To assess the influence of HFD on the architecture of enteric neuroglial network, fresh isolated distal ileum 10-cm segments were rinsed with Krebs solution to remove any contents and fixed in 4% paraformaldehyde (PFA) in PBS for 2 h at room temperature. After three subsequent 30-minutes washes with PBS, ileal segments were cut into 0.5-cm pieces opened along the mesenteric border and placed as a flat sheet to the bottom of Sylgard-coated dishes, with the mucosal side down. Using a dissecting microscope, longitudinal muscle–myenteric plexus (LMMP) whole-mount preparations were isolated as previously described [54]. LMMP preparations from all experimental groups were pinned down on the bottom of Sylgard-coated dishes and washed in PBS with 0.3% Triton X-100 (PBT) for 45 min with gentle shaking. After blocking nonspecific-binding sites with 5% bovine serum albumin (BSA) in PBT for 1.5 h at room temperature, LMMPs were incubated overnight at room temperature with primary antibodies (**Table 1**) diluted in PBT and 5% BSA. The following day, LMMPs were washed with PBT and incubated for 2 hours at room temperature with the secondary antibodies (**Table 1**), diluted in PBT and BSA 5%. LMMP preparations were then mounted on glass slides using a Mowiol mounting medium (CitiFluor™ Mountant Solution AF1) and stored in the dark at -20°C until analysis. Negative controls were obtained by incubating sections with isotype-matched control antibodies at the same concentration as the primary antibody and/or preincubating each antibody with the corresponding control peptide (final concentration as indicated by the manufacturer's instructions). The immunorelated procedures used comply with the recommendations made by the British Society of Pharmacology [55].

Table 1. Primary and secondary antibodies and their respective dilutions used for immunohistochemistry on ileal whole-mount preparations.

Antibody	Host Species	Dilution	Catalog Number	Source
Primary Antisera (Clone)				
HuC/D (monoclonal)	Mouse biotin-conjugated	1:100	A-21272	Thermo Fisher Scientific
nNOS (polyclonal)	Rabbit	1:100	61-700	Thermo Fisher Scientific
GFAP (polyclonal)	Chicken	1:100	ab4674	Abcam
S100β (polyclonal)	Guinea pig	1:100	ab10353	Abcam
ChAT (polyclonal)	Goat	1:50	AB144P	Sigma-Aldrich
Secondary Antisera				
Donkey anti-goat IgY Alexa 555-conjugated	-	1:500	A-21432	Thermo Fisher Scientific
Streptavidin Alexa 555-conjugated	-	1:1000	S21381	Thermo Fisher Scientific
Streptavidin Alexa 488-conjugated	-	1:1000	S11223	Thermo Fisher Scientific
Goat anti-Chicken IgY Alexa 488 conjugated	-	1:1000	A-11039	Thermo Fisher Scientific
Goat anti-Guinea Pig IgG Alexa 488 conjugated	-	1:1000	A-11073	Thermo Fisher Scientific
Goat anti-Rabbit IgG Alexa 488-conjugated	-	1:1000	A-11008	Thermo Fisher Scientific

 doi:10.20944/preprints202506.2222.v1

4.7.2. Confocal Image Acquisition and Analysis

Images were acquired with a Zeiss LSM 800 confocal imaging system (Oberkoken, Germany) equipped with a 20x objective or an oil-immersion 63× objective (NA 1.4), as previously described [19]. Briefly, Z-series images (25 planes) of 512 x 512 pixels were captured and processed as maximum intensity projections for LMMP whole-mount preparations. All microscope settings were kept constant for all images. In LMMPs, the analysis of total neurons in myenteric ganglia was performed by counting the number of HuC/D$^+$ cells in 10 randomly chosen images per mouse and normalized to the area of the ganglia. To evaluate the distribution of nitrergic neurons in ileal myenteric plexus, the number of nNOS$^+$ enteric neurons was blindly counted and normalized as described before[16,26]. Fluorescence intensity (density index) of GFAP, S100β and ChAT was determined in LMMP whole mount preparation by measuring the fluorescent intensity for each antigen in 10 images captured randomly in the ileal neuromuscular compartment per mouse (N = 5 mice/group), as previously reported [20,26,56]. The intensity of staining for each antibody was expressed as the density index of labeling normalized per myenteric ganglion area and was reported as mean ± SEM. All image analyses were performed using ImageJ (Fiji) Version Number 1.54i.

4.8. RNA Isolation and Quantitative RT-PCR

Total RNA was extracted from mice mucosa-deprived small intestine samples with TRIzol (Invitrogen, Carlsbad, CA, USA) and treated with DNase I (DNase Free, Ambion) to remove possible traces of contaminating DNA. Two μg of total RNA was retrotranscribed using the High-Capacity cDNA synthesis kit (Applied Biosystems, Life Technologies, Grand Island, NY, USA). Quantitative RT-PCR was performed on the QuantStudio 3 Real-Time PCR Systems (Thermo Fisher Scientific, Carlsbad, California) with Power Sybr Green Universal PCR Master Mix (Applied Biosystems, Foster City, CA, USA) following manufacturer's instructions. Primers were designed to have a similar amplicon size and similar amplification efficiency as required for the utilization of the 2-ΔΔCt method to compare gene expression [56], using Primer Express software (Applied Biosystems, Foster City, CA, USA) based on available sequences deposited in public database. Primer sequences are the following: IL-6 (F 5′-TAGTCCTTCCTACCCCAATTTCC-3′; R 5′-TTGGTCCTTAGCCACTCCTTC-3′); IL-1β (F 5′-GCAACTGTTCCTGAACTCAACT-3′; R 5′-ATCTTTTGGGGTCCGTCAACT-3′); TNFα (F 5′-CCCTCACACTCAGATCATCTTCT-3′; R 5′-GCTACGACGTGGGCTACAG-3′). For quantitative RT-PCR, a final concentration of 500 nm for each primer was used and experiments were performed in at least seven different biological samples for each experimental group (n=5), as previously described [57]. $2^{-\Delta\Delta Ct}$ values obtained from the comparison between normalized Ct values of HFD-treated samples with those obtained from SHAM were used to evaluate the effect of HFD-induced obesity on the expression of pro-inflammatory cytokines.

4.9. High-Performance Liquid Chromatography (HPLC) Analysis of 5-HT Levels

Ileal 5-HT level was analysed on tissue homogenates by HPLC, as pre viously described [19]. Briefly, freshly isolated ileal segments were immersed in liquid nitrogen and pulverized in a cooled stainless mortar containing 1 N $HClO_4$ (0.5 ml). The homogenates were then sonicated with an Elmasonic S30 sonica tor (Elma, Singer). After centrifugation (13,000 g for 30 min at 4°C), the supernatants were stored at 80C until HPLC analysis, whereas the pellets were dissolved in 1 N NaOH and boiled for 20 min at 60°C and then centrifuged at 15,000 g for 10 min at 4C. The isolated supernatants were used for protein determination. The supernatants were brought to about pH 4–5 with 1 N NaOH and analysed using a HPLC system (Shimadzu LC-10AD, Italy) equipped with a fluorometric detector (Shimadzu RF-10AXL) set at the excitation and emission wavelengths of 285 and 345 nm, respectively. Briefly, chromato graphic separation of tryptophan metabolites was performed using an analytical Apollo EPS C18 100A column (5 μm; 250 4.6 mm; Grace, Deerfield, IL, USA) and an Alltech guard column with stationary-phase RP-8 (25 to 40 μm LiChroprep; Merck Darmstadt). Kynurenine analy sis was carried out on an analytical Grace Smart RP-18 column (5 μm;

 doi:10.20944/preprints202506.2222.v1

250 4.6mm; Grace) using an ultraviolet–visible (UV–Vis) detector (SPD-10A, Shimadzu), set at 360 nm. The mobile phases were as fol lows: Phase A, 95% acetonitrile–5% water, and Phase B, 90% water 5%methanol (pH 3.8). The analyte elution was performed with an iso cratic gradient (5% Phase A and 95% Phase B, v/v) at 1 mlmin 1 flow rate.

4.10. Chemicals

Unless otherwise specified, all chemicals were obtained from Sigma–Aldrich (Milan, Italy) and were of the highest commercially available analytical grade. PFA and mounting solution (Citifluor AF1) were purchased from Electron Microscopy Sciences-Società Italiana Chimici (Rome, Italy), and Triton-X-100 was obtained from Applichem (Milan, Italy). All drugs for in vitro contractility studies were dissolved in Milli-Q water.

4.11. Statistical Analysis

All data are expressed as mean ± SEM except for the geometric centre, which is presented as median and range (minimum–maximum). All the results were analyzed by investigators blinded to the treatments using GraphPad Prism software Version 8.4 (San Diego, CA, USA). Animals were randomly divided into four experimental groups. The distribution of data was tested with the Shapiro–Wilk normality test. Statistical significance was calculated with a paired or unpaired Student's t test for two-sample comparisons, a two-way analysis of variance (ANOVA) followed by a Bonferroni post hoc test for multiple comparisons, or the non-parametric Mann–Whitney U-test for independent variables.

The differences between groups were considered significant when $P<0.05$; 'N' values indicate the number of animals. Post hoc tests were run only if F achieved $P<0.05$ and there was no significant variance inhomogeneity. The data and statistical analysis in this study comply with the recommendations on experimental design and analysis in pharmacology [47,49].

5. Conclusions

The intricate pathogenesis of enteric neuropathy in obesity arises from the interplay of multiple factors, which must be identified and evaluated as potential pharmacological targets. Overall, our findings underscore the critical role of TLR4 signaling in mediating the deleterious effects of a high-fat diet on the morpho-functional integrity of the ENS. A deeper understanding of the neuroimmune interactions within the gut will be the key to developing more effective therapeutic strategies and facilitating the translation of preclinical findings into clinical applications.

Author Contributions: S.F.: conceptualization, data curation, formal analysis, investigation, methodology, writing—original draft preparation, writing—review and editing; S.C.: conceptualization, data curation, formal analysis, investigation, methodology, writing—original draft preparation, writing—review and editing; A.B.: investigation, formal analysis, methodology; C.G.: conceptualization, funding acquisition, methodology, project administration, supervision, writing—original draft preparation, writing—review and editing; E.N.: investigation, methodology, writing—review and editing; E.V.S.: conceptualization, funding acquisition, supervision, writing—original draft preparation, writing—review and editing; C.P.: conceptualization, methodology, writing—review and editing; L.A.: conceptualization, methodology, writing—review and editing; V.C.: conceptualization, formal analysis, methodology, supervision, writing—original draft preparation, writing—review and editing; M.C.G.: conceptualization, data curation, formal analysis, funding acquisition, methodology, project administration, supervision, writing—original draft preparation, writing—review and editing. All authors have read and agreed to the published version of the manuscript.

Funding: This study was supported by grants from University of Padova to M.C.G (San Camillo Hospital Grant, Treviso (Italy); UNIPD-DSF-PRID-2023; AlfaWassermann spa VC2016SC2019AW), to S.F. (MUR/University of Padova PhD Fellowship 2020; Department of Pharmaceutical and Pharmacological Sciences PostDoc Fellowship ARD-B 2023; Department of Pharmaceutical and Pharmacological Sciences PostDoc Fellowship ARD-A 2024),

 doi:10.20944/preprints202506.2222.v1

and to S.C. (Department of Pharmaceutical and Pharmacological Sciences PostDoc Fellowship ARD-B 2020; ECCO Grant 2022).

Institutional Review Board Statement: The experiments complied with the national and EU guidelines for animal use in biomedical research. The animal study protocol was approved by the University of Padova Animal Care and Use Ethics Committee and by the Italian Ministry of Health (authorization number: 1142/2015-PR and 624/2021-PR).

Data Availability Statement: The datasets and materials used and/or analyzed during the currentstudy are available from the corresponding author upon reasonable request.

Acknowledgments: This study was supported by grants from University of Padova to M.C.G (San Camillo Hospital Grant, Treviso (Italy); UNIPD-DSF-PRID-2023; AlfaWassermann spa VC2016SC2019AW), to S.F. (MUR/University of Padova PhD Fellowship 2020; Department of Pharmaceutical and Pharmacological Sciences PostDoc Fellowship ARD-B 2023; Department of Pharmaceutical and Pharmacological Sciences PostDoc Fellowship ARD-A 2024), and to S.C. (Department of Pharmaceutical and Pharmacological Sciences PostDoc Fellowship ARD-B 2020; ECCO Grant 2022). The funders had no role in the design of the study; in the collection, analyses, or interpretation of data; in the writing of the manuscript; or in the decision to publish the results. The authors would like to thank Francesca Patrese, DMV, and Ludovico Scenna, DMV (University of Padova, Padova, Italy), for veterinary assistance, Alessia Forgiarini, Andrea Pagetta, Carla Argentini and Massimo Rizza (University of Padova, Padova, Italy) for technical assistance in animal handling and experimental procedures.

Conflicts of Interest: E.V.S. has served as speaker for Abbvie, Abivax, Agave, AGPharma, Alfasigma, CaDiGroup, Celltrion, Dr Falk, EG Stada Group, Fenix Pharma, Galapagos, Johnson&Johnson, JB Pharmaceuticals, Innovamedica/Adacyte, Eli Lilly, Malesci, Mayoly Biohealth, Omega Pharma, Pfizer, Reckitt Benckiser, Sandoz, SILA, Sofar, Takeda, Tillots, Unifarco; has served as consultant for Abbvie, Agave, Alfasigma, Biogen, Bristol-Myers Squibb, Celltrion, Dr. Falk, Eli Lilly, Fenix Pharma, Johnson&Johnson, JB Pharmaceuticals, Merck & Co, Nestlè, Pfizer, Reckitt Benckiser, Regeneron, Sanofi, SILA, Sofar, Takeda, Unifarco; he received research support from Bonollo, Difass, Pfizer, Reckitt Benckiser, SILA, Sofar, Unifarco, Zeta Farmaceutici. The Authors have no affiliations with organizations that have direct or indirect financial interests in the topic or materials covered in the manuscript. The funders had no role in the design of the study; in the collection, analyses, or interpretation of data; in the writing of the manuscript; or in the decision to publish the results.

Abbreviations

The following abbreviations are used in this manuscript:

5-HT	Serotonin
CCh	Carbachol
ChAT	Choline acetyltransferase
EFS	Electric field stimulation
EGCs	Enteric glial cells
ENS	Enteric nervous system
GFAP	Glial fibrillary acidic protein
HFD	High-fat diet
iNOS	Inducible NOS
LMMP	Longitudinal-muscle myenteric plexus
nNOS	Neuronal NOS
SD	Standard diet
TLRs	Toll-like receptors

References

1. Collaborators, G.B.D.A.B. Global, regional, and national prevalence of adult overweight and obesity, 1990-2021, with forecasts to 2050: a forecasting study for the Global Burden of Disease Study 2021. *Lancet* **2025**, *405*, 813-838, doi:10.1016/S0140-6736(25)00355-1.

 doi:10.20944/preprints202506.2222.v1

2. Bhattarai, Y.; Fried, D.; Gulbransen, B.; Kadrofske, M.; Fernandes, R.; Xu, H.; Galligan, J. High-fat diet-induced obesity alters nitric oxide-mediated neuromuscular transmission and smooth muscle excitability in the mouse distal colon. *Am J Physiol Gastrointest Liver Physiol* **2016**, *311*, G210-220, doi:10.1152/ajpgi.00085.2016.
3. Astrup, A.; Dyerberg, J.; Selleck, M.; Stender, S. Nutrition transition and its relationship to the development of obesity and related chronic diseases. *Obes Rev* **2008**, *9 Suppl 1*, 48-52, doi:10.1111/j.1467-789X.2007.00438.x.
4. Ellulu, M.S.; Patimah, I.; Khaza'ai, H.; Rahmat, A.; Abed, Y. Obesity and inflammation: the linking mechanism and the complications. *Arch Med Sci* **2017**, *13*, 851-863, doi:10.5114/aoms.2016.58928.
5. Khan, S.; Luck, H.; Winer, S.; Winer, D.A. Emerging concepts in intestinal immune control of obesity-related metabolic disease. *Nat Commun* **2021**, *12*, 2598, doi:10.1038/s41467-021-22727-7.
6. D'Antongiovanni, V.; Benvenuti, L.; Fornai, M.; Pellegrini, C.; van den Wijngaard, R.; Cerantola, S.; Giron, M.C.; Caputi, V.; Colucci, R.; Hasko, G.; et al. Glial A(2B) Adenosine Receptors Modulate Abnormal Tachykininergic Responses and Prevent Enteric Inflammation Associated with High Fat Diet-Induced Obesity. *Cells* **2020**, *9*, doi:10.3390/cells9051245.
7. Almeida, P.P.; Valdetaro, L.; Thomasi, B.B.M.; Stockler-Pinto, M.B.; Tavares-Gomes, A.L. High-fat diets on the enteric nervous system: Possible interactions and mechanisms underlying dysmotility. *Obes Rev* **2022**, *23*, e13404, doi:10.1111/obr.13404.
8. D'Antongiovanni, V.; Pellegrini, C.; Fornai, M.; Colucci, R.; Blandizzi, C.; Antonioli, L.; Bernardini, N. Intestinal epithelial barrier and neuromuscular compartment in health and disease. *World J Gastroenterol* **2020**, *26*, 1564-1579, doi:10.3748/wjg.v26.i14.1564.
9. Fried, S.; Wemelle, E.; Cani, P.D.; Knauf, C. Interactions between the microbiota and enteric nervous system during gut-brain disorders. *Neuropharmacology* **2021**, *197*, 108721, doi:10.1016/j.neuropharm.2021.108721.
10. D'Antongiovanni, V.; Fornai, M.; Colucci, R.; Nericcio, A.; Benvenuti, L.; Di Salvo, C.; Segnani, C.; Pierucci, C.; Ippolito, C.; Nemeth, Z.H.; et al. Enteric glial NLRP3 inflammasome contributes to gut mucosal barrier alterations in a mouse model of diet-induced obesity. *Acta Physiol (Oxf)* **2025**, *241*, e14232, doi:10.1111/apha.14232.
11. Thaiss, C.A.; Levy, M.; Grosheva, I.; Zheng, D.; Soffer, E.; Blacher, E.; Braverman, S.; Tengeler, A.C.; Barak, O.; Elazar, M.; et al. Hyperglycemia drives intestinal barrier dysfunction and risk for enteric infection. *Science* **2018**, *359*, 1376-1383, doi:10.1126/science.aar3318.
12. Mamun, M.A.A.; Rakib, A.; Mandal, M.; Singh, U.P. Impact of a High-Fat Diet on the Gut Microbiome: A Comprehensive Study of Microbial and Metabolite Shifts During Obesity. *Cells* **2025**, *14*, doi:10.3390/cells14060463.
13. Anitha, M.; Reichardt, F.; Tabatabavakili, S.; Nezami, B.G.; Chassaing, B.; Mwangi, S.; Vijay-Kumar, M.; Gewirtz, A.; Srinivasan, S. Intestinal dysbiosis contributes to the delayed gastrointestinal transit in high-fat diet fed mice. *Cell Mol Gastroenterol Hepatol* **2016**, *2*, 328-339, doi:10.1016/j.jcmgh.2015.12.008.
14. Reichardt, F.; Baudry, C.; Gruber, L.; Mazzuoli, G.; Moriez, R.; Scherling, C.; Kollmann, P.; Daniel, H.; Kisling, S.; Haller, D.; et al. Properties of myenteric neurones and mucosal functions in the distal colon of diet-induced obese mice. *J Physiol* **2013**, *591*, 5125-5139, doi:10.1113/jphysiol.2013.262733.
15. Kim, H.J.; Kim, H.; Lee, J.H.; Hwangbo, C. Toll-like receptor 4 (TLR4): new insight immune and aging. *Immun Ageing* **2023**, *20*, 67, doi:10.1186/s12979-023-00383-3.
16. Caputi, V.; Marsilio, I.; Cerantola, S.; Roozfarakh, M.; Lante, I.; Galuppini, F.; Rugge, M.; Napoli, E.; Giulivi, C.; Orso, G.; et al. Toll-Like Receptor 4 Modulates Small Intestine Neuromuscular Function through Nitrergic and Purinergic Pathways. *Front Pharmacol* **2017**, *8*, 350, doi:10.3389/fphar.2017.00350.
17. Anitha, M.; Vijay-Kumar, M.; Sitaraman, S.V.; Gewirtz, A.T.; Srinivasan, S. Gut microbial products regulate murine gastrointestinal motility via Toll-like receptor 4 signaling. *Gastroenterology* **2012**, *143*, 1006-1016 e1004, doi:10.1053/j.gastro.2012.06.034.
18. Ochoa-Cortes, F.; Ramos-Lomas, T.; Miranda-Morales, M.; Spreadbury, I.; Ibeakanma, C.; Barajas-Lopez, C.; Vanner, S. Bacterial cell products signal to mouse colonic nociceptive dorsal root ganglia neurons. *Am J Physiol Gastrointest Liver Physiol* **2010**, *299*, G723-732, doi:10.1152/ajpgi.00494.2009.
19. Faggin, S.; Cerantola, S.; Caputi, V.; Tietto, A.; Stocco, E.; Bosi, A.; Ponti, A.; Bertazzo, A.; Macchi, V.; Porzionato, A.; et al. Toll-like receptor 4 deficiency ameliorates experimental ileitis and enteric neuropathy:

 doi:10.20944/preprints202506.2222.v1

Involvement of nitrergic and 5-hydroxytryptaminergic neurotransmission. *Br J Pharmacol* **2025**, *182*, 1803-1822, doi:10.1111/bph.17439.

20. Cerantola, S.; Caputi, V.; Marsilio, I.; Ridolfi, M.; Faggin, S.; Bistoletti, M.; Giaroni, C.; Giron, M.C. Involvement of Enteric Glia in Small Intestine Neuromuscular Dysfunction of Toll-Like Receptor 4-Deficient Mice. *Cells* **2020**, *9*, doi:10.3390/cells9040838.
21. Kim, K.A.; Gu, W.; Lee, I.A.; Joh, E.H.; Kim, D.H. High fat diet-induced gut microbiota exacerbates inflammation and obesity in mice via the TLR4 signaling pathway. *PLoS One* **2012**, *7*, e47713, doi:10.1371/journal.pone.0047713.
22. Reichardt, F.; Chassaing, B.; Nezami, B.G.; Li, G.; Tabatabavakili, S.; Mwangi, S.; Uppal, K.; Liang, B.; Vijay-Kumar, M.; Jones, D.; et al. Western diet induces colonic nitrergic myenteric neuropathy and dysmotility in mice via saturated fatty acid- and lipopolysaccharide-induced TLR4 signalling. *J Physiol* **2017**, *595*, 1831-1846, doi:10.1113/JP273269.
23. Holland, W.L.; Bikman, B.T.; Wang, L.P.; Yuguang, G.; Sargent, K.M.; Bulchand, S.; Knotts, T.A.; Shui, G.; Clegg, D.J.; Wenk, M.R.; et al. Lipid-induced insulin resistance mediated by the proinflammatory receptor TLR4 requires saturated fatty acid-induced ceramide biosynthesis in mice. *J Clin Invest* **2011**, *121*, 1858-1870, doi:10.1172/JCI43378.
24. Cingolani, F.; Balasubramaniam, A.; Srinivasan, S. Molecular mechanisms of enteric neuropathies in high-fat diet feeding and diabetes. *Neurogastroenterol Motil* **2024**, e14897, doi:10.1111/nmo.14897.
25. Nezami, B.G.; Mwangi, S.M.; Lee, J.E.; Jeppsson, S.; Anitha, M.; Yarandi, S.S.; Farris, A.B., 3rd; Srinivasan, S. MicroRNA 375 mediates palmitate-induced enteric neuronal damage and high-fat diet-induced delayed intestinal transit in mice. *Gastroenterology* **2014**, *146*, 473-483 e473, doi:10.1053/j.gastro.2013.10.053.
26. Caputi, V.; Marsilio, I.; Filpa, V.; Cerantola, S.; Orso, G.; Bistoletti, M.; Paccagnella, N.; De Martin, S.; Montopoli, M.; Dall'Acqua, S.; et al. Antibiotic-induced dysbiosis of the microbiota impairs gut neuromuscular function in juvenile mice. *Br J Pharmacol* **2017**, *174*, 3623-3639, doi:10.1111/bph.13965.
27. Beraldi, E.J.; Soares, A.; Borges, S.C.; de Souza, A.C.; Natali, M.R.; Bazotte, R.B.; Buttow, N.C. High-fat diet promotes neuronal loss in the myenteric plexus of the large intestine in mice. *Dig Dis Sci* **2015**, *60*, 841-849, doi:10.1007/s10620-014-3402-1.
28. Stenkamp-Strahm, C.M.; Kappmeyer, A.J.; Schmalz, J.T.; Gericke, M.; Balemba, O. High-fat diet ingestion correlates with neuropathy in the duodenum myenteric plexus of obese mice with symptoms of type 2 diabetes. *Cell Tissue Res* **2013**, *354*, 381-394, doi:10.1007/s00441-013-1681-z.
29. Soares, A.; Beraldi, E.J.; Ferreira, P.E.; Bazotte, R.B.; Buttow, N.C. Intestinal and neuronal myenteric adaptations in the small intestine induced by a high-fat diet in mice. *BMC Gastroenterol* **2015**, *15*, 3, doi:10.1186/s12876-015-0228-z.
30. Capoccia, E.; Cirillo, C.; Gigli, S.; Pesce, M.; D'Alessandro, A.; Cuomo, R.; Sarnelli, G.; Steardo, L.; Esposito, G. Enteric glia: A new player in inflammatory bowel diseases. *Int J Immunopathol Pharmacol* **2015**, *28*, 443-451, doi:10.1177/0394632015599707.
31. Bertrand, R.L.; Senadheera, S.; Markus, I.; Liu, L.; Howitt, L.; Chen, H.; Murphy, T.V.; Sandow, S.L.; Bertrand, P.P. A Western diet increases serotonin availability in rat small intestine. *Endocrinology* **2011**, *152*, 36-47, doi:10.1210/en.2010-0377.
32. Kim, H.J.; Kim, J.H.; Noh, S.; Hur, H.J.; Sung, M.J.; Hwang, J.T.; Park, J.H.; Yang, H.J.; Kim, M.S.; Kwon, D.Y.; et al. Metabolomic analysis of livers and serum from high-fat diet induced obese mice. *J Proteome Res* **2011**, *10*, 722-731, doi:10.1021/pr100892r.
33. Mawe, G.M.; Hoffman, J.M. Serotonin signalling in the gut--functions, dysfunctions and therapeutic targets. *Nat Rev Gastroenterol Hepatol* **2013**, *10*, 473-486, doi:10.1038/nrgastro.2013.105.
34. Duan, Y.; Zeng, L.; Zheng, C.; Song, B.; Li, F.; Kong, X.; Xu, K. Inflammatory Links Between High Fat Diets and Diseases. *Front Immunol* **2018**, *9*, 2649, doi:10.3389/fimmu.2018.02649.
35. Jacobson, A.; Yang, D.; Vella, M.; Chiu, I.M. The intestinal neuro-immune axis: crosstalk between neurons, immune cells, and microbes. *Mucosal Immunol* **2021**, *14*, 555-565, doi:10.1038/s41385-020-00368-1.
36. Ye, L.; Li, G.; Goebel, A.; Raju, A.V.; Kong, F.; Lv, Y.; Li, K.; Zhu, Y.; Raja, S.; He, P.; et al. Caspase-11-mediated enteric neuronal pyroptosis underlies Western diet-induced colonic dysmotility. *J Clin Invest* **2020**, *130*, 3621-3636, doi:10.1172/JCI130176.

 doi:10.20944/preprints202506.2222.v1

37. Wang, H.; Foong, J.P.P.; Harris, N.L.; Bornstein, J.C. Enteric neuroimmune interactions coordinate intestinal responses in health and disease. *Mucosal Immunol* **2022**, *15*, 27-39, doi:10.1038/s41385-021-00443-1.
38. Velloso, L.A.; Folli, F.; Saad, M.J. TLR4 at the Crossroads of Nutrients, Gut Microbiota, and Metabolic Inflammation. *Endocr Rev* **2015**, *36*, 245-271, doi:10.1210/er.2014-1100.
39. Antonioli, L.; D'Antongiovanni, V.; Pellegrini, C.; Fornai, M.; Benvenuti, L.; di Carlo, A.; van den Wijngaard, R.; Caputi, V.; Cerantola, S.; Giron, M.C.; et al. Colonic dysmotility associated with high-fat diet-induced obesity: Role of enteric glia. *FASEB J* **2020**, *34*, 5512-5524, doi:10.1096/fj.201901844R.
40. Gulhane, M.; Murray, L.; Lourie, R.; Tong, H.; Sheng, Y.H.; Wang, R.; Kang, A.; Schreiber, V.; Wong, K.Y.; Magor, G.; et al. High Fat Diets Induce Colonic Epithelial Cell Stress and Inflammation that is Reversed by IL-22. *Sci Rep* **2016**, *6*, 28990, doi:10.1038/srep28990.
41. Schaeffler, A.; Gross, P.; Buettner, R.; Bollheimer, C.; Buechler, C.; Neumeier, M.; Kopp, A.; Schoelmerich, J.; Falk, W. Fatty acid-induced induction of Toll-like receptor-4/nuclear factor-kappaB pathway in adipocytes links nutritional signalling with innate immunity. *Immunology* **2009**, *126*, 233-245, doi:10.1111/j.1365-2567.2008.02892.x.
42. Manolakis, A.C.; Kapsoritakis, A.N.; Tiaka, E.K.; Sidiropoulos, A.; Gerovassili, A.; Satra, M.; Vamvakopoulou, D.; Tsiopoulos, F.; Papanas, N.; Skoularigis, I.; et al. TLR4 gene polymorphisms: evidence for protection against type 2 diabetes but not for diabetes-associated ischaemic heart disease. *Eur J Endocrinol* **2011**, *165*, 261-267, doi:10.1530/EJE-11-0280.
43. Kaya, S.D.; Sinen, O.; Bulbul, M. Gastric motor dysfunction coincides with the onset of obesity in rats fed with high-fat diet. *Clin Exp Pharmacol Physiol* **2021**, *48*, 553-562, doi:10.1111/1440-1681.13448.
44. Nyavor, Y.; Estill, R.; Edwards, H.; Ogden, H.; Heideman, K.; Starks, K.; Miller, C.; May, G.; Flesch, L.; McMillan, J.; et al. Intestinal nerve cell injury occurs prior to insulin resistance in female mice ingesting a high-fat diet. *Cell Tissue Res* **2019**, *376*, 325-340, doi:10.1007/s00441-019-03002-0.
45. Marsilio, I.; Caputi, V.; Latorre, E.; Cerantola, S.; Paquola, A.; Alcalde, A.I.; Mesonero, J.E.; O'Mahony, S.M.; Bertazzo, A.; Giaroni, C.; et al. Oxidized phospholipids affect small intestine neuromuscular transmission and serotonergic pathways in juvenile mice. *Neurogastroenterology and Motility* **2021**, *33*, doi:10.1111/nmo.14036.
46. Forcen, R.; Latorre, E.; Pardo, J.; Alcalde, A.I.; Murillo, M.D.; Grasa, L. Toll-like receptors 2 and 4 modulate the contractile response induced by serotonin in mouse ileum: analysis of the serotonin receptors involved. *Neurogastroenterol Motil* **2015**, *27*, 1258-1266, doi:10.1111/nmo.12619.
47. Curtis, M.J.; Alexander, S.; Cirino, G.; Docherty, J.R.; George, C.H.; Giembycz, M.A.; Hoyer, D.; Insel, P.A.; Izzo, A.A.; Ji, Y.; et al. Experimental design and analysis and their reporting II: updated and simplified guidance for authors and peer reviewers. *Br J Pharmacol* **2018**, *175*, 987-993, doi:10.1111/bph.14153.
48. McGrath, J.C.; Lilley, E. Implementing guidelines on reporting research using animals (ARRIVE etc.): new requirements for publication in BJP. *Br J Pharmacol* **2015**, *172*, 3189-3193, doi:10.1111/bph.12955.
49. Percie du Sert, N.; Hurst, V.; Ahluwalia, A.; Alam, S.; Avey, M.T.; Baker, M.; Browne, W.J.; Clark, A.; Cuthill, I.C.; Dirnagl, U.; et al. The ARRIVE guidelines 2.0: Updated guidelines for reporting animal research. *PLoS Biol* **2020**, *18*, e3000410, doi:10.1371/journal.pbio.3000410.
50. Antonioli, L.; Caputi, V.; Fornai, M.; Pellegrini, C.; Gentile, D.; Giron, M.C.; Orso, G.; Bernardini, N.; Segnani, C.; Ippolito, C.; et al. Interplay between colonic inflammation and tachykininergic pathways in the onset of colonic dysmotility in a mouse model of diet-induced obesity. *Int J Obes (Lond)* **2019**, *43*, 331-343, doi:10.1038/s41366-018-0166-2.
51. Brun, P.; Giron, M.C.; Qesari, M.; Porzionato, A.; Caputi, V.; Zoppellaro, C.; Banzato, S.; Grillo, A.R.; Spagnol, L.; De Caro, R.; et al. Toll-like receptor 2 regulates intestinal inflammation by controlling integrity of the enteric nervous system. *Gastroenterology* **2013**, *145*, 1323-1333, doi:10.1053/j.gastro.2013.08.047.
52. Giron, M.C.; Bin, A.; Brun, P.; Etteri, S.; Bolego, C.; Florio, C.; Gaion, R.M. Cyclic AMP in rat ileum: evidence for the presence of an extracellular cyclic AMP-adenosine pathway. *Gastroenterology* **2008**, *134*, 1116-1126, doi:10.1053/j.gastro.2008.01.030.

 doi:10.20944/preprints202506.2222.v1

53. Tuladhar, B.R.; Womack, M.D.; Naylor, R.J. Pharmacological characterization of the 5-HT receptor-mediated contraction in the mouse isolated ileum. *British Journal of Pharmacology* **2000**, *131*, 1716-1722, doi:https://doi.org/10.1038/sj.bjp.0703747.
54. Cerantola, S.; Faggin, S.; Annaloro, G.; Mainente, F.; Filippini, R.; Savarino, E.V.; Piovan, A.; Zoccatelli, G.; Giron, M.C. Influence of Tilia tomentosa Moench Extract on Mouse Small Intestine Neuromuscular Contractility. *Nutrients* **2021**, *13*, doi:10.3390/nu13103505.
55. Alexander, S.P.H.; Roberts, R.E.; Broughton, B.R.S.; Sobey, C.G.; George, C.H.; Stanford, S.C.; Cirino, G.; Docherty, J.R.; Giembycz, M.A.; Hoyer, D.; et al. Goals and practicalities of immunoblotting and immunohistochemistry: A guide for submission to the British Journal of Pharmacology. *Br J Pharmacol* **2018**, *175*, 407-411, doi:10.1111/bph.14112.
56. Cerantola, S.; Faggin, S.; Caputi, V.; Bosi, A.; Banfi, D.; Rambaldo, A.; Porzionato, A.; Di Liddo, R.; De Caro, R.; Savarino, E.V.; et al. Small intestine neuromuscular dysfunction in a mouse model of dextran sulfate sodium-induced ileitis: Involvement of dopaminergic neurotransmission. *Life Sci* **2022**, *301*, 120562, doi:10.1016/j.lfs.2022.120562.
57. Bistoletti, M.; Caputi, V.; Baranzini, N.; Marchesi, N.; Filpa, V.; Marsilio, I.; Cerantola, S.; Terova, G.; Baj, A.; Grimaldi, A.; et al. Antibiotic treatment-induced dysbiosis differently affects BDNF and TrkB expression in the brain and in the gut of juvenile mice. *PLoS One* **2019**, *14*, e0212856, doi:10.1371/journal.pone.0212856.